Genetic Variants of *ABCC10*, a Novel Tenofovir Transporter, Are Associated With Kidney Tubular Dysfunction

Sudeep P. Pushpakom,[1,2,a] Neill J. Liptrott,[1,2,a] Sonia Rodríguez-Nóvoa,[3] Pablo Labarga,[3] Vincent Soriano,[3] Marta Albalater,[3] Elizabeth Hopper-Borge,[4] Stefano Bonora,[5] Giovanni Di Perri,[5] David J. Back,[2] Saye Khoo,[1,2] Munir Pirmohamed,[1,2] and Andrew Owen[2]

[1]National Institute for Health Research Biomedical Research Centre, Royal Liverpool Hospital, and [2]Department of Pharmacology, University of Liverpool, United Kingdom; [3]Department of Infectious Diseases, Hospital Carlos III, Madrid, Spain; [4]Developmental Therapeutics Program, Fox Chase Cancer Center, Pennsylvania; and [5]Department of Infectious Diseases, University of Turin, Amedeo di Savoia Hospital, Italy

Background. Tenofovir (TFV) causes kidney tubular dysfunction (KTD) in some patients, but the mechanism is poorly understood. Genetic variants in TFV transporters are implicated; we explored whether *ABCC10* transports TFV and whether *ABCC10* single-nucleotide polymorphisms (SNPs) are associated with KTD.

Methods. TFV accumulation was assessed in parental and *ABCC10*-transfected HEK293 cells (HEK293-ABCC10), CD4$^+$ cells and monocyte-derived macrophages (MDMs). Substrate specificity was confirmed by cepharanthine (ABCC10 inhibitor) and small interfering RNA (siRNA) studies. Fourteen SNPs in *ABCC10* were genotyped in human immunodeficiency virus–positive patients with KTD ($n = 19$) or without KTD (controls; $n = 96$). SNP and haplotype analysis was performed using Haploview.

Results. TFV accumulation was significantly lower in HEK293-ABCC10 cell lines than in parental HEK293 cells (35% lower; $P = .02$); this was reversed by cepharanthine. siRNA knockdown of *ABCC10* resulted in increased accumulation of TFV in CD4$^+$ cells (18%; $P = .04$) and MDMs (25%; $P = .04$). Two *ABCC10* SNPs (rs9349256: odds ratio [OR], 2.3; $P = .02$; rs2125739, OR, 2.0; $P = .05$) and their haplotype (OR, 2.1; $P = .05$) were significantly associated with KTD. rs9349256 was associated with urine phosphorus wasting ($P = .02$) and β2 microglobulinuria ($P = .04$).

Conclusions. TFV is a substrate for *ABCC10*, and genetic variability within the *ABCC10* gene may influence TFV renal tubular transport and contribute to the development of KTD. These results need to be replicated in other cohorts.

Tenofovir (TFV) has high antiviral potency, low drug interaction potential, and a good safety profile [1]. Large prospective clinical trials have shown that TFV is relatively safe for the kidney [2, 3]. However, several reports have described kidney tubular dysfunction (KTD),

including Fanconi syndrome [4–7]. The incidence of KTD ranges from 1.4% [5] to 22% [6], triggering concern about long-term use of TFV. Underestimation of the prevalence of TFV-associated KTD has also been suggested, owing to the low sensitivity of diagnostic markers such as serum creatinine [8, 9].

Different mechanisms have been suggested for TFV-associated KTD, including interaction with drug transporters located in the renal tubule [10]. TFV is transported into proximal tubular cells by organic anion transporters (OAT1 and, to a lesser extent, OAT3), which are located on the basolateral membrane [11, 12]. Renal clearance of TFV occurs via a combination of glomerular filtration and active tubular secretion [10], but the luminal efflux systems involved in transport out of proximal tubular cells into the lumen are not well

studied. Only 2 efflux transporters, *ABCC4* (MRP4) [12, 13] and *ABCC2* (MRP2) [14] have been reported to play a role in the elimination of TFV.

A high degree of interindividual variability in disease characteristics and severity are seen with TFV-associated KTD [10], and genetic variants of various transporters have been investigated [15, 16]. Both *ABCC4* [15, 16] and *ABCC2* [15] variants were shown to be associated, but polymorphisms in other transporters such as *SLC22A6* and *ABCB1* were not [16]. In addition, old age [3, 16, 17] and lower body weight [3, 16] are also known risk factors. It is clear that KTD is multifactorial, and the genetic associations identified so far do not explain the large interindividual variability. It is likely that other transporters are involved in TFV transport and may play a role in KTD.

ABCC10 (MRP7) exhibits functional similarity to other ABCC transporters [18]. Recent studies have shown that *ABCC10* transports anticancer agents such as gemcitabine and taxanes from tumor cells and thereby confers drug resistance [19]. Antiretroviral agents, such as zalcitabine and 9-[2-phosphonylmethoxynyl]-adenine are also substrates for *ABCC10* [20]. *ABCC10* is ubiquitously expressed; a microarray of 50 transporters in 40 human tissues found high expression in tissues, including kidney, brain, and colon [21].

The current study was designed to investigate whether TFV was a substrate for ABCC10. In addition, high-throughput genotyping of *ABCC10* variants using Sequenom MALDI-TOF technology was employed in a cohort of TFV-treated human immunodeficiency virus (HIV)–positive patients to investigate whether genetic variants of *ABCC10* were associated with KTD susceptibility.

MATERIALS AND METHODS

Materials
Radiolabeled TFV was purchased from Moravek Biochemicals. Parental HEK293, *ABCC10*-transfected HEK293 cells (HEK293-*ABCC10*), and ABCC10 primary antibody were as described elsewhere [19]. Cepharanthine (*ABCC10* inhibitor) was purchased from Aktin Chemicals. Healthy volunteer buffy coats were obtained from the National Blood Service. CD4$^+$ and CD14$^+$ magnetic beads, macrophage colony-stimulating factor (M-CSF), and transforming growth factor β were purchased from Miltenyi Biotec. *ABCC10*, glyceraldehyde 3-phosphate dehydrogenase (GAPDH)–positive control and nontargeting negative control small interfering RNA (siRNA) were purchased from Dharmacon (Thermo Fisher). Lipofectamine RNAiMAX was purchased from Invitrogen. Taqman gene expression assay for *ABCC10* messenger RNA (mRNA) expression and Taqman Gene Expression Master Mix were purchased from Applied Biosystems. Sequence-specific polymerase chain reaction (PCR) primers and extend reaction oligonucleotides were obtained from Metabion GmbH.

Accumulation of Radiolabeled TFV in *ABCC10* Expressing Cell Lines
Tritiated TFV (.3 μCi/mL; 10 μmol) was incubated with parental HEK293 and HEK293-*ABCC10* (designated C17 and C18) cells for 30 min at 37°C. Lower drug concentrations are more likely to result in spurious findings, because transporters may be important only at subtherapeutic concentrations and may become saturated at higher concentrations; therefore, higher TFV concentration was chosen to ensure applicability of the data beyond the therapeutic plasma range. TFV was used instead of TFV disoproxil fumarate, because the latter is virtually undetectable in systemic circulation [22]. Samples were centrifuged at 9000 rpm for 1 min at 4°C–8°C, and supernatant (100 μL) representing the extracellular count was taken and placed into a scintillation vial. Pellets were resuspended in 1 mL of ice-cold Hank's balanced salt solution, centrifuged, resuspended in 100 μL of water to solubilize the cell pellet, and transferred into a separate scintillation vial. Scintillation fluid (4 mL) was added to each vial and placed in the scintillation counter. Data were expressed as the ratio of intracellular to extracellular drug, assuming a cell volume of 1 pL for calculating the cellular accumulation ratio. Accumulation experiments were conducted in the presence and absence of cepharanthine (2 μmol), an inhibitor of *ABCC10*, to confirm specificity.

Isolation of CD4$^+$ and CD14$^+$ Cells and Monocyte-Derived Macrophages
Immune cell subsets were isolated from peripheral blood mononuclear cells (PBMCs) using magnetic beads. Cells were resuspended in Miltenyi Biotec Product (MACS) buffer (phosphate-buffered saline, 0.5% bovine serum albumin, and 2 mmol/L ethylenediaminetetraacetic acid [EDTA]) and centrifuged, and pellets were resuspended in 80 μL of MACS buffer and 20 μL of MACS beads, specific for either CD4 or CD14, vortexed, and incubated for 15 min at 4°–8°C. Cells were then washed and resuspended in 500 μL of MACS buffer. MACS LS columns were placed in a magnetic field and primed with 3 mL of MACS buffer, and cell suspensions were added and washed through with MACS buffer solution. The columns were then removed from the magnetic field, and cells were harvested with 5 mL of MACS buffer and cultured in Roswell Park Memorial Institute (RPMI) 1640 medium containing 15% fetal calf serum (FCS).

For monocyte-derived macrophages (MDMs), PBMCs were cultured overnight in RPMI 1640 medium containing 15% FCS in order for monocytes to adhere. Media and lymphocytes were washed off with Hank's balanced salt solution, and monocytes were removed using trypsin-EDTA. CD14$^+$ cells were then separated using magnetic bead separation and cultured for 12 days in RPMI 1640 medium (20% FCS) containing M-CSF (10 ng/mL) and transforming growth factor β (10 ng/mL).

siRNA-Mediated Knockdown of *ABCC10* Expression in Primary CD4⁺ Cells and MDMs

Expression of *ABCC10* mRNA in various immune cell subsets was ascertained by TaqMan Assays on Demand (assay ID, Hs00375716_m1) using real-time quantitative PCR. siRNA specific for *ABCC10* mRNA, along with the relevant nontargeting (negative) and GAPDH-specific (positive) controls, was transfected into CD4⁺ cells and MDMs using RNAiMAX under optimum conditions. Gene expression relative to β-actin (assay ID, 4352935E) expression was calculated using the comparative Ct (cycle time) method, as described elsewhere [23]. Protein expression for *ABCC10* was determined by flow cytometry as described elsewhere [24], using *ABCC10* primary antibody and isotype control (immunoglobulin G) at 1:40 dilutions. A goat anti-mouse fluorescein isothiocyanate–conjugated secondary antibody was used at a 1:200 dilution.

Patients

The characteristics of the study population have been described elsewhere [16]. Briefly, the study population was drawn from HIV-infected patients receiving TFV-containing therapy at a single clinic in Madrid during the first trimester of 2008 [6]. Local research ethics committee approvals were obtained for the study. Written informed consent was obtained from all patients for collection of blood/DNA samples and subsequent genetic analysis. The criteria used for diagnosis of KTD in this cohort have been described elsewhere [16]. A total of 115 HIV-infected patients were examined; 96 of them did not show evidence of KTD (control group), and 19 had KTD (KTD group).

Quantification of Plasma TFV Levels

Mid-dose TFV plasma concentration was available for a subset of patients ($n = 76$; 63 controls and 13 patients with KTD) who overlapped with the patient cohort reported by Rodriguez-Novoa et al [25]; these concentrations were measured using a validated high-performance liquid chromatography-mass spectrometry method [26] by our collaborators in Turin. Time sample was between 10 and 14 h.

Selection of Single-Nucleotide Polymorphisms in *ABCC10*

Fourteen SNPs in *ABCC10* were selected for screening, including 7 haplotype-tagging single-nucleotide polymorphisms (htSNPs) from the CEPH/CEU (Centre d'Etude du Polymorphisme Humain/ Utah residents with Northern and Western European ancestry) HapMap data set (phase II, release 23a; March 2008) using Haploview software (http://www.broad.mit.edu/haploview/haploview). The criteria used for single-nucleotide polymorphism (SNP) selection included a minor allele frequency of >5% and pairwise linkage disequilibrium measure of $r^2 > 0.8$. Marker coverage for *ABCC10* was extended by 5000 base pairs upstream and downstream flanking regions to include any potential regulatory SNPs. Apart from the htSNPs, we also selected 7 additional SNPs from the

dbSNP database (www.ncbi.nlm.nih.gov/projects/SNP/) that were either exonic or mapped to untranslated or conserved regions within the selected region and hence potentially functionally important. A graphic representation of the *ABCC10* gene and all the SNP markers genotyped is given in Figure 1.

Genotyping

DNA was extracted from PBMCs using a QIAamp DNA Mini Kit. SNP genotyping was performed using a Sequenom MassARRAY MALDI-TOF system. A multiplex SNP assay (14-plex) was designed using Sequenom software (https://mysequenom.com/tools/genotyping/default.aspx) and iPLEX chemistry with 10 ng of genomic DNA. For each assay, quality control procedures included use of replicate samples and negative template controls. Each SNP genotype cluster plot was manually checked and scored. Any sample with a call rate <80% and any assay with a call rate <90% were omitted.

Statistical Analysis

Distribution of the data was assessed using the Shapiro-Wilk test. Difference in accumulation of TFV between parental HEK293 and HEK293-*ABCC10* cell lines, difference in expression between siRNA-mediated knockdown samples and untreated samples, and difference in accumulation of TFV between immune cell subsets after siRNA-mediated knockdown of *ABCC10* were assessed using the Mann-Whitney test. Differences were considered significant at $P < .05$. Haploview software was used to test Hardy-Weinberg equilibrium, differences in allele and genotype frequencies between KTD and control groups for each SNP, and *ABCC10* haplotype analysis. The parameters used for linkage disequilibrium analysis are D′ and r^2 [27]. Multivariate analysis and associations between single renal parameters and *ABCC10* SNPs were analyzed by logistic regression using SPSS software (version 16.0) (method: forward stepwise: likelihood ratio). We used existing genotype data on *ABCC2* and *ABCC4* SNPs to carry out an extended haplotype analysis with the *ABCC10* SNPs, performed with Haploview software.

RESULTS

Accumulation of Radiolabeled TFV in *ABCC10*-Expressing Cell Lines

Accumulation of radiolabeled TFV was significantly lower in HEK293-*ABCC10* cell lines, C17 and C18, than in the parental
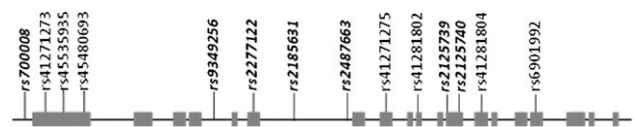
Figure 1. Graphic representation of *ABCC10* gene and single-nucleotide polymorphism (SNP) markers selected. Exons are represented by gray boxes. Approximate locations of SNP markers are shown. Haplotype tag SNPs are shown in bold italic type.

HEK293 cells (Figure 2) (35% lower than the parental cellular accumulation ratio in C17, $P = .02$; 31% lower than that in C18, $P = .02$), suggesting increased efflux of TFV in HEK293-ABCC10 cell lines. The addition of 2 μmol cepharanthine, an ABCC10 inhibitor, inhibited the efflux of TFV in HEK293-ABCC10 cells (Figure 2).

siRNA-Mediated Knockdown of ABCC10 Expression in CD4+ Cells and MDMs

ABCC10 mRNA was detectable in all immune cell subsets isolated from healthy volunteer peripheral blood. GAPDH siRNA was included as a positive control, with expression being normalized to β-actin. GAPDH mRNA was significantly lower in CD4+ cells (Figure 3a) (89.9% reduction; $P = .0004$) and MDMs (Figure 3b) (66.9% reduction; $P = .0006$) 48 h after transfection. ABCC10 mRNA was similarly reduced 48 h after transfection with ABCC10-specific siRNA in CD4+ cells (Figure 3a; 75.9% reduction, $P = .0006$) and MDMs (Figure 3b) (67.9% reduction; $P = .0006$) compared with untreated control cells. This reduction in expression was also observed when results were compared with those in the negative control transfected cells. ABCC10 protein levels were also significantly lower in CD4+ cells (82.3% reduction; $P = .0004$) and MDMs (68.5% reduction; $P = .007$) 48 h after transfection (Figures 3c and 3d, respectively). siRNA-mediated knockdown of ABCC10 expression resulted in a significant increase in the intracellular accumulation of radiolabeled TFV in MDMs (25% increase; $P = .04$) and CD4+ cells (18%; $P = .04$) compared with untreated control cells (Figure 3e and f), confirming the substrate specificity of ABCC10 for TFV.

Association of ABCC10 Polymorphisms With TFV-Related KTD

The clinical characteristics of the study cohort have been described elsewhere [16]. No statistically significant differences
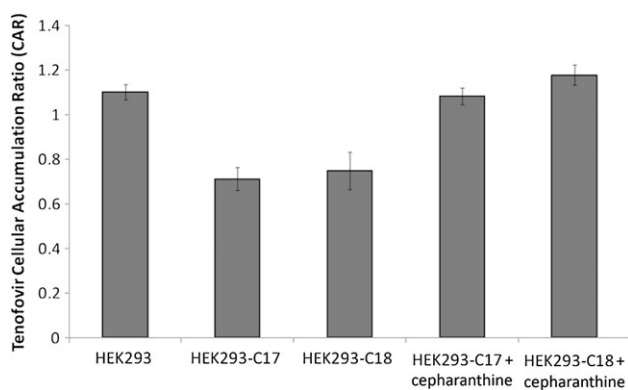
Figure 2. Accumulation of radiolabeled TFV in ABCC10-expressing cell lines. ABCC10-overexpressing cells C17 and C18 showed a significant reduction in the intracellular accumulation of tenofovir (TFV), suggesting ABCC10-mediated TFV efflux. Cepharanthine (2 μmol), a potent ABCC10 inhibitor, prevents this efflux. Data expressed as means ± standard deviations ($n = 6$).

were observed for demographic factors, use of protease inhibitors, duration of TFV therapy, or baseline biochemical parameters.

All SNP markers genotyped were in Hardy-Weinberg equilibrium. Single SNP analysis by Haploview identified one SNP marker in ABCC10 (rs9349256) to be significantly associated with KTD, and another marker (rs2125739) was marginally significantly associated (Table 1). The associated G allele of rs9349256 (located in intron 4) was significantly over-represented in the KTD group (72.2%; odds ratio [OR] 2.3; 95% confidence interval [CI], 1.1–5.3; $P = .02$) compared with the non-KTD controls (52.6%). rs2125739 is a nonsynonymous SNP located in exon 12 of ABCC10 and results in isoleucine-to-threonine conversion (p.Ile920Thr). The frequency of the variant C allele of rs2125739 was marginally significantly higher in the KTD group (38.8%; OR, 2.0; 95% CI, .9–4.4; $P = .05$) than in the control group (23.4%). Haplotype analysis of ABCC10 identified a 3-marker haplotype, GGC, consisting of associated alleles of both the above-described markers, to be marginally significantly more prevalent in patients with KTD than in the control group (38.9% in KTD vs 23% in non-KTD controls; OR, 2.1; 95% CI, .9–4.6; $P = .05$) (Table 1).

Association of ABCC10-ABCC2 Extended Haplotype With KTD

We have elsewhere shown an association between the ABCC2 SNP, rs717620 and its haplotype, CGTC (consisting of the associated rs717620C allele) with KTD [16]. Haploview was used to investigate the prevalence of the ABCC2 haplotype, CGTC, in combination with the associated ABCC10 haplotype, GGC (extended haplotype GGC-CGTC). The frequency of the ABCC10-ABCC2 extended haplotype was significantly higher in the KTD group than in the controls (22.1% vs 8.4%; OR, 3.0; 95% CI, 1.2–7.9; $P = .01$) (Table 2).

Association of ABCC10 SNPs and ABCC10−ABCC2 Extended Haplotype With KTD Parameters

Logistic regression analysis was conducted to identify whether any of the ABCC10 SNPs were associated with individual parameters of KTD. rs9349256 was significantly associated with 2 parameters: urine phosphorus wasting (OR, 1.9; $P = .02$; 95% CI, 1.1–3.4) and β2-microglobulinuria (OR, 1.7; $P = .04$; 95% CI, 1.1–3.7) (Table 3). In addition, the ABCC10−ABCC2 extended haplotype GGC-CGTC was independently associated with urine phosphorus wasting (OR, 2.6; $P = .02$; 95% CI, 1.1–5.9) (Table 3).

Association of KTD and ABCC10 SNPs With TFV Plasma Concentration

Median TFV plasma levels were significantly ($P = .006$) higher in patients with KTD (182 ng/mL; interquartile range, 19–259) than in controls (103 ng/mL; interquartile range, 81–410). Neither the ABCC10 SNPs nor the carriers of ABCC10-ABCC2 extended haplotype (GGC-CGTC) showed any association with
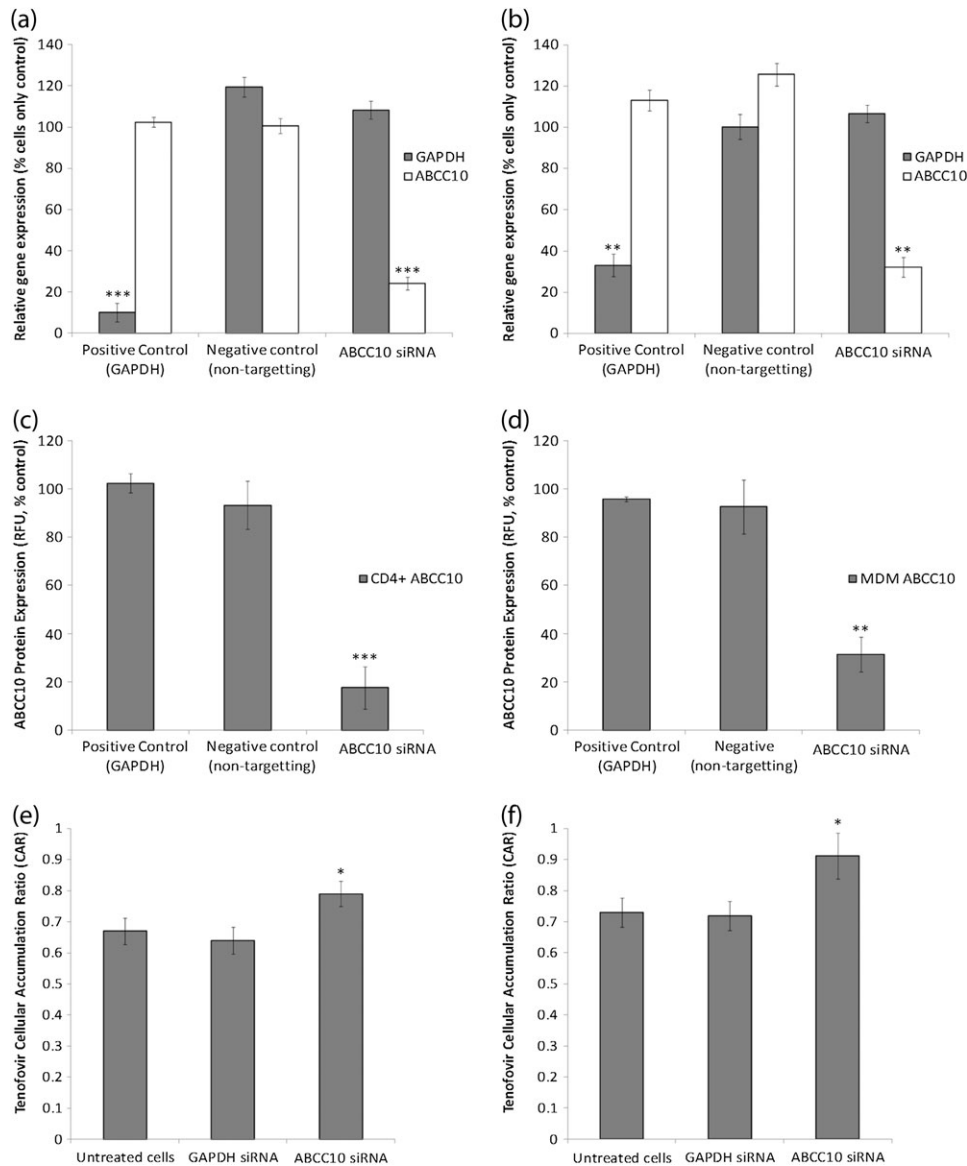
Figure 3. Knockdown of *ABCC10* in CD4+ T cells and monocyte-derived macrophages (MDMs) and accumulation of tenofovir (TFV) 48 h after knockdown. *A–D,* Expression of *ABCC10* messenger RNA in CD4+ cells (*A*) and MDMs (*B*) and of *ABCC10* protein in CD4+ cells (*C*) and MDMs (*D*), after small interfering RNA (siRNA)–mediated knockdown. GAPDH, glyceraldehyde 3-phosphate dehydrogenase. *E, F,* Accumulation of TFV is increased after knockdown in CD4+ cells (*E*) and MDMs (*F*). Data are expressed as means ± standard deviations ($n = 6$). *p<0.05; **p<0.01; ***p<0.01

TFV plasma concentration. However, a trend toward gene dose effect was noted with rs2125739 genotypes (median TFV plasma concentration for wild type, 102 ng/mL; heterozygotes, 112 ng/mL; mutant homozygotes, 146 ng/mL), even though it was statistically nonsignificant ($P = .6$) (Table 1 and Figure 1; online only).

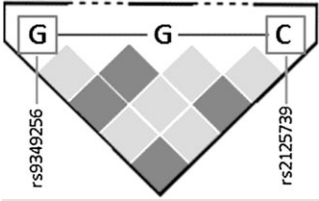### Independent Predictors of KTD in TFV-Treated HIV-Positive Patients

Multivariate analysis using a model including factors such as age, sex, duration of TFV therapy, body mass index, viral load, and carriage of GGC–CGTC haplotype identified age as the only significant predictor of KTD ($P = .04$) (Table 4). However, it

should be noted that the carriage of *ABCC10-ABCC2* extended haplotype and duration of TFV therapy only marginally missed the statistical threshold of significance ($P = .06$). TFV plasma levels were excluded from this model because our sample cohort did not have a complete record for all patients.

DISCUSSION

TFV was first approved by the FDA in 2001 and is currently a widely used antiretroviral agent [28]. However, KTD has been reported with long-term TFV use [4–7], with reported cases growing in number from 2 in 2002 [29, 30] to >15 in the last 2

Table 1. Allele Frequencies of rs9349256 and rs2125739 and Their Haplotype (GGC) in Control and Kidney Tubular Dysfunction (KTD) Groups

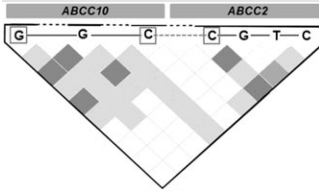| SNP marker/haplotype	Associated Allele	Allele/haplotype frequency, %		OR (95%CI)[a]	P
		Control group (n = 96)	KTD group (n = 19)		
rs9349256 (intron 4)	G	52.6	72.2	2.3 (1.1–5.3)	.02
rs2125739 (exon 12)	C	23.4	38.8	2.0 (.9–4.4)	.05
	GGC	23.0	38.9	2.1 (.9–4.6)	.05

NOTE. Linkage disequilibrium patterns within the *ABCC10* GGC haplotype are represented here. Dark gray shades indicate strong linkage disequilibrium; light gray shades, weak linkage disequilibrium. *ABCC10* GGC haplotype comprises rs9349256G, rs2487663G, and rs2125739C alleles. Independently associated alleles are highlighted in square boxes.

[a] Odds ratio (OR) and P values represent comparison of allele/haplotype frequencies between control and KTD groups. CI, confidence interval.

years, including several large scale studies [4, 6]. In a retrospective cross-sectional analysis of 1647 patients (964 on TFV-containing regimens, 683 on TFV-sparing regimens), TFV exposure was associated with a greater risk of developing proximal tubular dysfunction [4]. Importantly, adverse renal effects of TFV were also shown to persist.

Inhibition of renal efflux transporters may result in increased intracellular TFV, which in turn may cause renal toxicity. However, apart from a well-established role for ABCC4 [12, 13] and a tentative role for ABCC2 [14], no other transporters have been identified for TFV renal efflux. The recent discovery and characterization of ABCC10 [18], its functional similarity with ABCC4 [31], and its high expression in kidney [21] provided a rationale to explore its specificity for TFV and possible role in KTD.

Table 2. Comparison of *ABCC10−ABCC2* Extended Haplotype (GGC-CGTC) Frequency Between Control and Kidney Tubular Dysfunction (KTD) Groups

ABCC10−ABCC2 haplotype[a]	Frequency, %		OR (95% CI)[b]	P
	Control group	KTD group		
	8.4	22.1	3.0 (1.2–7.9)	.01

NOTE. [a] Linkage disequilibrium patterns within the *ABCC10−ABCC2* haplotype are represented here. Dark gray boxes indicate strong linkage disequilibrium; light gray and white boxes, weak linkage disequilibrium. The extended haplotype GGC-CGTC is defined by the *ABCC10* haplotype, GGC, and *ABCC2* haplotype, CGTC. Independently associated alleles in *ABCC10* and *ABCC2* are highlighted in square boxes.

[b] CI, confidence interval; OR, odds ratio.

The *ABCC10*-expressing embryonic kidney cell lines, C17 and C18, were used to establish that TFV is a substrate for ABCC10; the same in vitro models have elsewhere been used to characterize the transport of other substrates [18–20]. Furthermore, cepharanthine resulted in an increased intracellular accumulation of TFV, illustrating the importance of ABCC10 for TFV in renally derived cells. To assess the importance of ABCC10 at more physiologically relevant expression levels, siRNA experiments were conducted in CD4^{+} cells and MDMs. CD4^{+} cells and MDMs represent primary cell types that are readily available in large numbers and express transporters at physiologically relevant densities. They also allow assessment of the role of transporters in an HIV replication–competent cell system. Intracellular accumulation of radiolabeled TFV was significantly increased in siRNA-treated immune cells compared with untreated controls. Hence, the experimental evidence obtained in this study confirms a role for ABCC10 in the efflux transport of TFV.

A case-control association study was then undertaken to investigate common variants in *ABCC10* in HIV-positive patients on TFV-containing regimens. This is the first genetic association analysis reported for *ABCC10*. Two SNPs and their haplotype were significantly associated with KTD: rs9349256 located in intron 4 and rs2125739, a nonsynonymous SNP, in exon 12, resulting in an amino acid change (p.Ile920Thr). A recent study showed carriers of the *ABCC4* 3463G variant (associated elsewhere with KTD [15]) to have 35% higher intracellular TFV [32]. The functional effects of polymorphisms identified in *ABCC10* in this study are not known; a bioinformatic approach using FastSNP software (http://fastsnp.ibms.sinica.edu.tw/) found rs2125739 to be located in a putative splice site. Splice site polymorphisms have been shown to affect premRNA splicing and may cause the splicing apparatus to use nearby cryptic splice sites or skip exons, leading to an altered protein [33]. Based on HapMap data (www.hapmap.org), the

Table 3. Association Between Markers of Kidney Tubular Dysfunction (KTD) and Single-Nucleotide Polymorphism (SNP) Markers in *ABCC10* and *ABCC2* and Their Extended Haplotype

Gene and SNP marker/haplotype	Associated markers of KTD	OR (95% CI)[a]	*P*
ABCC10			
rs9349256	Urine phosphorus wasting	1.9 (1.1−3.4)	.02
	β2-microglobulinuria	1.7 (1.1−3.7)	.04
ABCC2[b]			
rs717620	Urine phosphorus wasting; β2-microglobulinuria		
rs2273697	Aminoaciduria		
rs3740066	β2-microglobulinuria		
ABCC10-ABCC2			
GGC-CGTC[c]	Urine phosphorus wasting	2.6 (1.1−5.9)	.02

NOTE. [a] CI, confidence interval; OR, odds ratio.

[b] Taken from our previous study on *ABCC2* and KTD [16], which identified association between 3 markers and various parameters of tubular dysfunction: rs717620 with urine phosphorus wasting and β2-microglobulinuria, rs2273697 with aminoaciduria, and rs3740066 with β2-microglobulinuria.

[c] Extended haplotype GGC-CGTC is defined by *ABCC10* haplotype, GGC, and *ABCC2* haplotype, CGTC.

minor allele frequency for rs2125739 in various populations are as follows: Northern and Western European ancestry (26.7%); Sub-Saharan African (34.2%); Han Chinese (3.4%), and Japanese (8.0%). No functional effect was predicted for rs9349256, suggesting that the association may be due to linkage

Table 4. Univariate and Multivariate Analysis for Factors Associated With Kidney Tubular Dysfunction in Human Immuno-deficiency Virus–Positive Patients Treated With Tenofovir (TFV)

Covariate	R^2	Univariate *P*	Multivariate *P*
rs700008	NA[a]	.3	…
rs41271273	NA	.6	…
rs45535935	NA	.2	…
rs45480693	NA	.6	…
rs9349256	NA	.02[b]	…
rs2277122	NA	.4	…
rs2185631	NA	.3	…
rs2487663	NA	.4	…
rs41271275	NA	…	…
rs41281802	NA	.6	…
rs2125739	NA	.05[b]	…
rs2125740	NA	.5	…
rs41281804	NA	…	…
rs6901992	NA	…	…
GGC-CGTC haplotype carriage	.02	.01[b]	.06[c]
Age	.1	.06	.04[b]
Sex	.03	.4	.2
Duration of therapy	.02	.2	.06
Body mass index	.2	.8	.7
TFV plasma levels	.3	.006[b]	Not included[d]
Viral load	.2	.3	.3

NOTE. [a] NA, not applicable.

[b] Significant differences ($P < .05$)

[c] GGC-CGTC carriage was included in the multivariate model instead of individual *ABCC10* single-nucleotide polymorphisms.

[d] TFV plasma levels were not included in the multivariate model because they were available only for a subset of patients.

disequilibrium with another functional marker. A marginally significant increase in the frequency of the haplotype defined by the 2 associated alleles was also observed in KTD compared with controls, further strengthening a role for *ABCC10* in TFV-associated KTD.

TFV-associated KTD is multifactorial [10] with risk factors including polymorphisms along with nongenetic factors, such as age [3, 16, 17] and body weight [3, 16]. The previous study using the same cohort found an association between KTD and *ABCC2* rs717620 and a haplotype containing it [16]. Therefore, the joint contribution of *ABCC10* and *ABCC2* haplotypes was investigated. The combination haplotype, GGC-CGTC, was significantly more prevalent in patients with KTD than in controls. The *ABCC10-ABCC2* combined haplotype was more strongly associated with KTD (OR, 3.0) than the individual haplotypes (OR, 2.1 and 1.96 for *ABCC10* and *ABCC2*, respectively). Interestingly, in a multivariate analysis, the carriage of *ABCC10-ABCC2* combined haplotype showed a trend toward independent significant association ($P = .06$) with KTD.

Median TFV plasma levels were significantly higher in a subset of patients with KTD than in controls, but they did not show any association with *ABCC10* SNPs or *ABCC10-ABCC2* combined haplotype. Smaller sample size could be one reason for the lack of association observed here; the relationship therefore needs to be explored in larger cohort studies. However, it is important to note that it is unclear whether the increase in TFV plasma levels observed in KTD is the cause or the consequence of the alterations in the tubular cells. Moreover, the intracellular kidney concentrations for TFV could be more important than the plasma TFV levels in the pathogenesis of KTD; it remains to be explored whether *ABCC10* polymorphisms are associated with intracellular TFV levels.

ABCC10 rs9349256 was associated with urine phosphorus wasting and β2-microglobulinuria. The *ABCC10-ABCC2* combination haplotype was also more prevalent in patients with

abnormal urine phosphorus excretion. This is interesting, because reports have suggested that fractional excretion of urine phosphate [5] and urinary β2-microglobulin [34] are more sensitive markers of tubular dysfunction than conventional markers. Conventional markers, such as serum creatinine and urine albumin, are primarily indicators of glomerular disease [8, 9, 34]. Urinary β2-microglobulin is freely filtered at the glomerulus and is avidly taken up and catabolized by the proximal renal tubules. Therefore, high levels of this protein indicate various pathologic conditions involving the proximal renal tubule. Urine phosphorus wasting is among the 3 criteria defining Fanconi syndrome. TFV is the drug most associated with this syndrome [35], which leads to bone demineralization and osteomalacia [36].

These results confirm that *ABCC10* is involved in the efflux transport of TFV. Renal elimination is the dominant mode of TFV clearance, and these findings add to our understanding of the molecular pharmacology of TFV. *ABCC10* mRNA has been found to be highly expressed in various tissues including kidney, brain and colon, suggesting an important role for this protein in the transport of drugs and other endogenous molecules. However, it is unclear whether *ABCC10* is expressed on the luminal or basolateral side of the tubular cell. We have also identified a role for *ABCC10* genetic variants in the pathogenesis of KTD using a limited sample size; replication of these results in an independent disease cohort is now required to validate these findings. Nevertheless, the findings of this study improves our understanding of genetic susceptibility factors involved in KTD pathogenesis and therefore may help in the development of avoidance strategies (stratification of medicines and better drug design) and intervention strategies (cotherapies to prevent manifestations of KTD).

Funding

References

1. Gallant JE, DeJesus E, Arribas JR, et al. Tenofovir DF, emtricitabine, and efavirenz vs. zidovudine, lamivudine, and efavirenz for HIV. N Engl J Med **2006**; 354:251–60.
2. Izzedine H, Hulot JS, Vittecoq D, et al. Long-term renal safety of tenofovir disoproxil fumarate in antiretroviral-naive HIV-1-infected patients. Data from a double-blind randomized active-controlled multicentre study. Nephrol Dial Transplant **2005**; 20:743–6.
3. Nelson MR, Katlama C, Montaner JS, et al. The safety of tenofovir disoproxil fumarate for the treatment of HIV infection in adults: the first 4 years. AIDS **2007**; 21:1273–81.
4. Horberg M, Tang B, Towner W, et al. Impact of tenofovir on renal function in HIV-infected, antiretroviral-naive patients. J Acquir Immune Defic Syndr **2010**; 53:62–9.
5. Izzedine H, Harris M, Perazella MA. The nephrotoxic effects of HAART. Nat Rev Nephrol **2009**; 5:563–73.
6. Labarga P, Barreiro P, Martin-Carbonero L, et al. Kidney tubular abnormalities in the absence of impaired glomerular function in HIV patients treated with tenofovir. AIDS **2009**; 23:689–96.
7. Peyriere H, Reynes J, Rouanet I, et al. Renal tubular dysfunction associated with tenofovir therapy: report of 7 cases. J Acquir Immune Defic Syndr **2004**; 35:269–73.
8. Hall AM, Edwards SG, Lapsley M, et al. Subclinical tubular injury in HIV-infected individuals on antiretroviral therapy: a cross-sectional analysis. Am J Kidney Dis **2009**; 54:1034–42.
9. Woodward CL, Hall AM, Williams IG, et al. Tenofovir-associated renal and bone toxicity. HIV Med **2009**; 10:482–7.
10. Rodriguez-Novoa S, Labarga P, Soriano V. Pharmacogenetics of tenofovir treatment. Pharmacogenomics **2009**; 10:1675–85.
11. Cihlar T, Ho ES, Lin DC, Mulato AS. Human renal organic anion transporter 1 (hOAT1) and its role in the nephrotoxicity of antiviral nucleotide analogs. Nucleosides Nucleotides Nucleic Acids **2001**; 20:641–8.
12. Ray AS, Cihlar T, Robinson KL, et al. Mechanism of active renal tubular efflux of tenofovir. Antimicrob Agents Chemother **2006**; 50:3297–304.
13. Imaoka T, Kusuhara H, Adachi M, Schuetz JD, Takeuchi K, Sugiyama Y. Functional involvement of multidrug resistance-associated protein 4 (MRP4/ABCC4) in the renal elimination of the antiviral drugs adefovir and tenofovir. Mol Pharmacol **2007**; 71:619–27.
14. Mallants R, Van Oosterwyck K, Van Vaeck L, Mols R, De Clercq E, Augustijns P. Multidrug resistance-associated protein 2 (MRP2) affects hepatobiliary elimination but not the intestinal disposition of tenofovir disoproxil fumarate and its metabolites. Xenobiotica **2005**; 35:1055–66.
15. Izzedine H, Hulot JS, Villard E, et al. Association between ABCC2 gene haplotypes and tenofovir-induced proximal tubulopathy. J Infect Dis **2006**; 194:1481–91.
16. Rodriguez-Novoa S, Labarga P, Soriano V, et al. Predictors of kidney tubular dysfunction in HIV-infected patients treated with tenofovir: a pharmacogenetic study. Clin Infect Dis **2009**; 48:e108–16.
17. Madeddu G, Bonfanti P, De Socio GV, et al. Tenofovir renal safety in HIV-infected patients: results from the SCOLTA Project. Biomed Pharmacother **2008**; 62:6–11.
18. Chen ZS, Hopper-Borge E, Belinsky MG, Shchaveleva I, Kotova E, Kruh GD. Characterization of the transport properties of human multidrug resistance protein 7 (MRP7, ABCC10). Mol Pharmacol **2003**; 63:351–8.
19. Hopper-Borge E, Chen ZS, Shchaveleva I, Belinsky MG, Kruh GD. Analysis of the drug resistance profile of multidrug resistance protein 7 (ABCC10): resistance to docetaxel. Cancer Res **2004**; 64:4927–30.
20. Hopper-Borge E, Xu X, Shen T, Shi Z, Chen ZS, Kruh GD. Human multidrug resistance protein 7 (ABCC10) is a resistance factor for nucleoside analogues and epothilone B.. Cancer Res **2009**; 69: 178–84.
21. Bleasby K, Castle JC, Roberts CJ, et al. Expression profiles of 50 xenobiotic transporter genes in humans and pre-clinical species: a resource for investigations into drug disposition. Xenobiotica **2006**; 36:963–88.
22. Kearney BP, Flaherty JF, Shah J. Tenofovir disoproxil fumarate: clinical pharmacology and pharmacokinetics. Clin Pharmacokinet **2004**; 43:595–612.
23. Liptrott NJ, Penny M, Bray PG, et al. The impact of cytokines on the expression of drug transporters, cytochrome P450 enzymes and chemokine receptors in human PBMC. Br J Pharmacol **2009**; 156:497–508.
24. Liptrott NJ, Khoo SH, Back DJ, Owen A. Detection of ABCC2, CYP2B6 and CYP3A4 in human peripheral blood mononuclear cells using flow cytometry. J Immunol Methods **2008**; 339:270–4.
25. Rodriguez-Novoa S, Labarga P, D'Avolio A, et al. Impairment in kidney tubular function in patients receiving tenofovir is associated with higher tenofovir plasma concentrations. AIDS **2010**; 24:1064–6.
26. D'Avolio A, Sciandra M, Siccardi M, et al. A new assay based on solid-phase extraction procedure with LC-MS to measure plasmatic

concentrations of tenofovir and emtricitabine in HIV infected patients. J Chromatogr Sci **2008**; 46:524–8.

27. Daly MJ, Rioux JD, Schaffner SF, Hudson TJ, Lander ES. High-resolution haplotype structure in the human genome. Nat Genet **2001**; 29:229–32.

28. Jimenez-Nacher I, Garcia B, Barreiro P, et al. Trends in the prescription of antiretroviral drugs and impact on plasma HIV-RNA measurements. J Antimicrob Chemother **2008**; 62:816–22.

29. Coca S, Perazella MA. Rapid communication: acute renal failure associated with tenofovir: evidence of drug-induced nephrotoxicity. Am J Med Sci **2002**; 324:342–4.

30. Verhelst D, Monge M, Meynard JL, et al. Fanconi syndrome and renal failure induced by tenofovir: a first case report. Am J Kidney Dis **2002**; 40:1331–3.

31. Kruh GD, Guo Y, Hopper-Borge E, Belinsky MG, Chen ZS. ABCC10, ABCC11, and ABCC12. Pflugers Arch **2007**; 453:675–84.

32. Kiser JJ, Aquilante CL, Anderson PL, King TM, Carten ML, Fletcher CV. Clinical and genetic determinants of intracellular tenofovir diphosphate concentrations in HIV-infected patients. J Acquir Immune Defic Syndr **2008**; 47:298–303.

33. ElSharawy A, Hundrieser B, Brosch M, et al. Systematic evaluation of the effect of common SNPs on pre-mRNA splicing. Hum Mutat **2009**; 30:625–32.

34. Gatanaga H, Tachikawa N, Kikuchi Y, et al. Urinary beta2-microglobulin as a possible sensitive marker for renal injury caused by tenofovir disoproxil fumarate. AIDS Res Hum Retroviruses **2006**; 22:744–8.

35. Izzedine H, Isnard-Bagnis C, Hulot JS, et al. Renal safety of tenofovir in HIV treatment-experienced patients. AIDS **2004**; 18:1074–6.

36. Earle KE, Seneviratne T, Shaker J, Shoback D. Fanconi's syndrome in HIV+ adults: report of three cases and literature review. J Bone Miner Res **2004**; 19:714–21.